

Distribution of Lattice Constants in CePt₃Si observed by Larmor Diffraction and SANS

R Ritz¹, S Mühlbauer¹, C Pfeleiderer¹, T Keller², J White³, M Laver³,
E M Forgan³, R Cubitt⁴, C Dewhurst⁴, P G Niklowitz⁵, A Prokofiev⁶
and E Bauer⁶

¹Physik Department E21, TU München, D-85748 Garching, Germany

²MPI für Festkörperforschung, Heisenbergstr. 1, D-70569 Stuttgart, Germany

³School of Physics and Astronomy, University of Birmingham, Birmingham B15 2TT, UK

⁴Institut Laue-Langevin, BP 156, F-38042 Grenoble, France

⁵Dep. of Physics, Royal Holloway, University of London, Egham TW20 0EX, UK

⁶Fakultät für Physik, Institut für Festkörperphysik, TU Wien, 1040 Wien, Austria

E-mail: Robert.Ritz@frm2.tum.de

Abstract. The non-centrosymmetric heavy fermion compound CePt₃Si orders antiferromagnetically at $T_N = 2.2$ K, followed by a superconducting transition, where $T_s = 0.45$ K for high quality samples and $T_s = 0.75$ K for lower quality samples. We have used neutron Larmor diffraction to measure the temperature dependence and distribution of the lattice constants in a single crystal of CePt₃Si with $T_s = 0.75$ K. In our study we observe an unusually wide range of lattice parameters for the a-axis and c-axis with $\Delta a/a \approx \Delta c/c \approx 10^{-3}$. Small angle neutron scattering suggests an abundance of defects along the lattice planes. When taking into account the pressure dependence of T_s our study attributes the increased value of T_s in low quality samples to an effective negative pressure.

1. Introduction

In recent years a large number of f-electron heavy fermion superconductors have been discovered that are prime candidates for non-electron-phonon pairing mechanisms and unconventional pairing symmetries [1]. A prominent example is the non-centrosymmetric f-electron compound CePt₃Si [2, 3]. At ambient pressure CePt₃Si orders antiferromagnetically below $T_N = 2.2$ K. Initial studies in polycrystals revealed an additional superconducting transition at $T_s = 0.75$ K, where the general phenomenology of CePt₃Si suggests the formation of heavy-fermion superconductivity in the vicinity of a quantum critical point. Under hydrostatic pressure the antiferromagnetism in CePt₃Si is suppressed above a critical pressure of $p_N = 8$ kbar, while the superconductivity vanishes above $p_s \approx 16$ kbar [4]. Motivated by the non-centrosymmetric crystal structure of CePt₃Si the most promising scenario for the superconducting pairing appears to be a chiral mixing of s- plus p-wave symmetry [5].

However, recently single-crystals of CePt₃Si have been grown by the Bridgman technique with much sharper anomalies in the specific heat at the antiferromagnet and superconducting transitions and lower normal state residual resistivity suggesting much better sample quality. Yet, the superconducting transition temperature in these samples was found to be reduced to $T_s = 0.45$ K [6]. Because unconventional superconductivity is well known to respond very

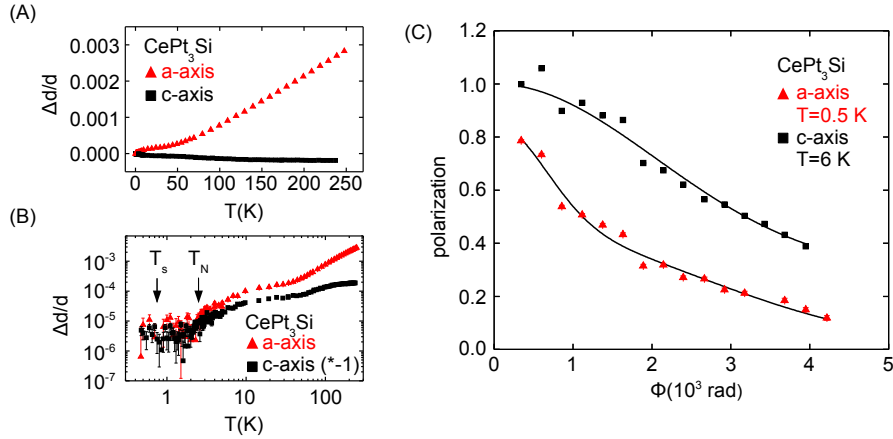


Figure 1. (A) $\Delta d/d$ of CePt_3Si as a function of temperature for the a - and the c -axis. (B) The same data shown as a double logarithmic plot. The c -axis data was multiplied by -1 for logarithmic display. The arrows indicate $T_N = 2.2$ K and $T_s = 0.75$, K. (C) Polarization as a function of total Larmor phase. Red triangles correspond to data measured for $[3, 0, 0]$ at 0.5 K, black squares correspond to data measured for $[0, 0, 4]$ at 6 K. The strong decrease of polarization is due to a large distribution of lattice constants $\Delta G/G \approx 10^{-3}$ in both directions.

sensitively to both magnetic and non-magnetic defects, this raises the question, why samples of seemingly better quality have a *reduced* superconducting transition temperature.

2. Experimental Method

In order to clarify the sample dependence of T_s in CePt_3Si we have measured the temperature dependence of the lattice constants and the distribution of lattice constants in a single crystal of CePt_3Si by means of neutron Larmor diffraction (LD), supplemented by small angle neutron scattering (SANS). For a detailed introduction to Larmor diffraction we refer to Ref. [7] and references therein. By comparison with standard neutron and x-ray scattering techniques Larmor diffraction provides an unprecedented high resolution of $\Delta d/d \approx 10^{-6}$. However, in comparison with standard capacitive dilatometry, which provides a resolution as high as $\Delta d/d \approx 10^{-10}$, the resolution of Larmor diffraction is low. Larmor diffraction is nevertheless unique, because (i) it represents a direct microscopic measurement of the lattice constant, (ii) it allows to determine the distribution of lattice constants, and (iii) it permits measurements under extreme conditions [8].

The principle of operation of Larmor diffraction is based on encoding the lattice spacing by the total Larmor phase of precession Φ_{tot} , given by

$$\Phi_{tot} = \frac{2\omega_L L m}{\pi \hbar} d \quad (1)$$

where ω_L is the Larmor precession frequency and L is the distance the neutrons travel between two pairs of neutron resonance spin echo (NRSE) coils before and after the sample. Thus changes of lattice constant lead to small changes of the total phase of precession $\Delta\Phi = \Phi_{tot}\Delta d/d$. As a unique feature LD allows to infer the distribution of lattice constants from the loss of beam polarization as a function of increasing Larmor frequency. For a Gaussian distribution of lattice constants with a full width at half maximum $\epsilon_{FW} = \Delta G/G$ the polarization varies as follows

$$P(\Phi_{tot}) = P_0 \exp\left(-\frac{\Phi_{tot}^2}{16 \ln 2} \epsilon_{FW}^2\right) \quad (2)$$

where G is the value of the reciprocal lattice vector.

Our Larmor diffraction measurements were carried out at the polarized thermal triple axis spectrometer TRISP at the neutron source Heinz Maier-Leibnitz (FRM II) at Technische Universität München. A ^3He -insert combined with a Closed Cycle Cryostat (CCR) was used for measurements down to 0.45 K. The measurements of the a- and c-axis were conducted on the $[3, 0, 0]$ and $[0, 0, 4]$ Bragg peaks, respectively, using neutrons with an incident and final wave vector of $k_i = k_f = 2.83 \text{ \AA}^{-1}$. Effective Larmor frequencies of 800 kHz and 1000 kHz were used for measurements of the lattice constants as a function of temperature. For measurements of the distribution of lattice constants the effective Larmor frequencies were swept from 120 kHz up to 1196 kHz corresponding to total Larmor phases Φ_{tot} from 343.8 up to 4218.9. The small angle neutron scattering was carried out at D22 at the ILL, using neutrons with a wavelength $\lambda \approx 8 \text{ \AA} \pm 5\%$. The SANS measurements served originally as a search for a superconducting flux line lattice.

The large single crystal of CePt_3Si studied was grown in Vienna by optical float-zoning. Prior to our measurements the sample was characterized by Laue x-ray diffraction and A.C. susceptibility measurements, which established the single crystallinity of the sample and a very broad superconducting transition below $T_s \approx 0.75 \text{ K}$ (not shown), respectively. Measurements of the elastic scattering intensity at $[0, 0, 1/2]$ as a function of temperature moreover confirmed the onset of antiferromagnetic order at $T_N \approx 2.2 \text{ K}$.

3. Results and Discussion

Shown in Fig. 1 is the relative change of lattice constant $\Delta d/d$ as a function of temperature for the a- and the c-axis with respect to the value measured at the lowest temperatures available. To the best of our knowledge the thermal expansion of single-crystal CePt_3Si has not been reported before (studies of polycrystals under pressure are reported in Ref. [9]). Evidently the thermal expansion of CePt_3Si is highly anisotropic, where the a-axis decreases with decreasing temperature, while the c-axis increases by a tiny amount. The data for the c-axis shown in Fig. 1(B) has been multiplied by -1. The broad shoulder in the temperature dependence around several ten K is consistent with dominant energy scales related to the crystal field excitations and Kondo screening, previously inferred from other bulk properties [3].

Fig.1(C) shows the polarization of the signal for the a- and the c-axis as a function of total Larmor phase. Our data are best explained by invoking the presence of two Gaussian distributions of lattice constants, where $P(\Phi_{tot}) = w P_1(\Phi_{tot}) + (1 - w) P_2(\Phi_{tot})$ with $\epsilon_1 = \Delta G/G_1$, $\epsilon_2 = \Delta G/G_2$ and a weighting factor w . For the a-axis we found values of $w_a \approx 0.46$, $\Delta G/G_{a1} \approx 3.7 \cdot 10^{-3}$ and $\Delta G/G_{a2} \approx 0.9 \cdot 10^{-3}$, and for the c-axis $w_c \approx 0.71$, $\Delta G/G_{c1} \approx 1.2 \cdot 10^{-3}$ and $\Delta G/G_{c2} < 10^{-5}$. Overall this implies a similarly large distribution of the planes, where a detailed discussion of the differences is outside the scope of this paper.

The wide distribution of lattice constants seen in LD may be interpreted as a wide range of microscopic pressures Δp across the sample volume. For a first estimate of we consider $\Delta p = K \Delta V/V$. Taking the modulus of compressibility of copper $K_{\text{Cu}} = 125 \cdot 10^9 \text{ N/m}^2$ we find $\Delta p \approx 4 \text{ kbar}$. In combination with the pressure dependence of T_s observed experimentally we obtain $\Delta T_s \approx 0.15 \text{ K}$, where we infer dT_s/dp from the published $T - p$ -phase diagram of CePt_3Si [4]. However, if the distribution of effective internal pressures would be due to defects and metallurgical segregations on microscopic scales, one would expect that unconventional superconductivity is strongly suppressed.

To supplement the LD data we show in Fig. 2(A) a typical intensity pattern recorded in small angle neutron scattering at D22. We find strong scattering intensity along the crystallographic a-axis (see label in Fig.2(A)). At first sight, one might attribute this intensity pattern to the diffraction by large scale structures. However, closer inspection of the intensity variation as a function of wave vector and scattering angle 2θ seen in rocking scans with respect to a vertical

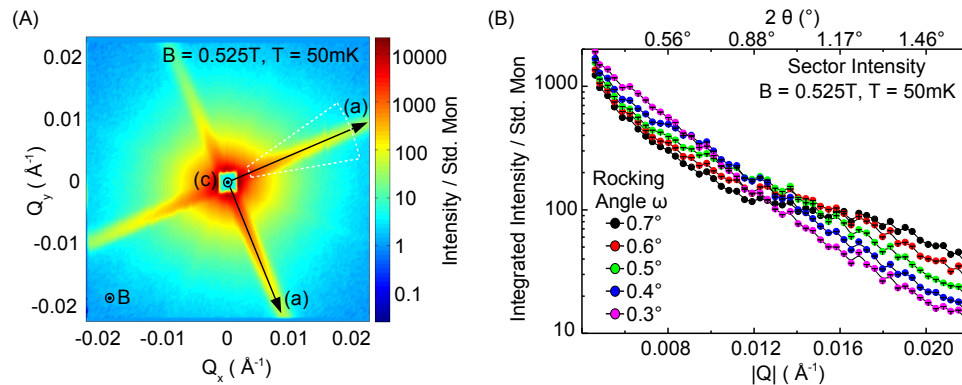


Figure 2. (A) Small angle neutron scattering intensity pattern for the intermediate quality single crystal of CePt_3Si investigated in our study. An abundance of scattering is observed along the ac-lattice planes, where the a- and c-axis are labelled as (a) and (c), respectively. (B) Scattering intensity in the sector shown in panel (A) as a function of wave vector or scattering angle 2θ for various rocking angles. The variation of the intensity as a function rocking angle ω is characteristic of reflections rather than small angle diffraction.

axis (rocking angle ω) suggests that considerable intensity shifts from large scattering angles to small scattering angles with decreasing ω (see Fig. 2(B)). This behavior is atypical of simple small angle diffraction. Rather it is the signature of an abundance of reflections confined to the crystallographic ac-plane. We have not studied the tetragonal basal plane, but expect the same to occur there.

As a possible explanation for the sample dependence of T_s the SANS data suggest, e.g., the presence of fissures parallel to the lattice planes causing reflections. The associated q -values suggest that these fissures may be quite large, exceeding the superconducting coherence length. In turn this suggests, that the material is comparatively free of defects on microscopic scales while the fissures may generate local strains. This supports the view that the superconductivity in CePt_3Si is indeed unconventional, even though T_s is lower in higher quality samples. Further microscopic studies will now have to identify the precise nature of the defects. This will pave the way to single-crystal growth of large high quality samples as a precondition for studies of the superconducting flux line lattice.

Acknowledgments

We wish to thank the staff at FRMII and the ILL for support during the experiments. SM acknowledges financial support through the EU COST program P16. CP acknowledges financial support through DFG (PF393/10). EB is grateful to the Austrian FWF, P18054.

References

- [1] C Pfeleiderer, Rev. Mod. Phys., in press, arXiv/0905.2625
- [2] Bauer E, et al. 2004 *Phys. Rev. Lett.* **92** 027003
- [3] Bauer E, et al. 2007 *J. Phys. Soc. Jpn.* **76** 051009
- [4] Nicklas M, Sparn G, Lackner R, Bauer E and Steglich F 2005 *Physica B* **359** 386
- [5] Frigeri P A, Agterberg D F, Koga A and Sigrist M 2005 *Physica B* **359** 371
- [6] Takeuchi T, et al. *J. Phys. Soc. Jpn.* **76** 014702
- [7] Rekveldt M T, Keller T and Golub R 2001 *Eur. Phys. Lett.* **54** 342–346
- [8] Pfeleiderer C, Böni P, Keller T, Rößler U K and Rosch A 2007 *Science* **316** 1871
- [9] Ohashi M, Oomi G, Nakano T and Umatoko Y 2006 *Physica B* **378-380** 379